Assignment 6: Explain the Periodic Table

Marta Casado Carrasquer

May 14, 2025

1 Introduction

In this assignment, we aim to develop a self-consistent mean-field approach to approximate the behaviour of atomic systems by reducing the full many-body problem to a set of one-electron equations.

We combine methods used in previous assignments in order to build our implementation. The radial Schrödinger equation is solved iteratively, with the electronic potential updated through the Poisson equation for the direct Coulomb interaction and an approximate exchange potential using the Slater expression.

We test our model for different atomic systems: **He**, $\mathbf{He}^+$, **Ne**, $\mathbf{Ne}^+$, **Ar**, $\mathbf{Ar}^+$, and **K**, $\mathbf{K}^+$.

2 Theory and Methods

2.1 Self-Consistent Mean-Field Model

The objective for this assignment is to approximate the many-electron problem by a mean-field model. We aim to reduce the full many-body problem to a set of one-particle radial Schrödinger equations which are solved self-consistently.

As seen in previous assignments, $P_{n\ell}(r)$ satisfies the radial Schrödinger equation in Hartree atomic units:

$$\left[-\frac{1}{2}\frac{d^2}{dr^2} + \frac{\ell(\ell+1)}{2r^2} - \frac{Z}{r} + V_{ee}(r)\right] P_{n\ell}(r) = E_{n\ell} P_{n\ell}(r) \tag{1}$$

where $V_{ee}(r)$ is the electronic potential corresponding to all other electrons. This potential has a direct Coulomb term and an exchange part (Slater potential).

2.2 B-Spline and Knot Sequence

To solve the radial Schrödinger equation numerically, we follow the same procedure as in Assignment 5 and expand $P_{n\ell}(r)$ in a B-spline basis which we define on a knot sequence from $r = 0$ to $r = r_{\max}$. We again implement the same boundary conditions where we remove the first and last splines: $P_{n\ell}(0) = P_{n\ell}(r_{\max}) = 0$.

The knot sequence of choice is constructed by concatenating a linear grid from $r = 0$ to r_{cut} with an exponential grid from $[r_{\text{cut}}, r_{\max}]$, just as in Assignment 5:

$$\texttt{knots} = \texttt{linspace}(0, r_{\text{cut}}, N_{\text{linear}}) \cup \left[r_{\text{cut}} + (r_{\max} - r_{\text{cut}}) \frac{\exp(s) - 1}{\exp(1) - 1} \right]_{s \in [0,1]}.$$

2.3 Matrix Representation

We again end up with a generalized eigenvalue problem:

$$\mathbf{Hc} = E_{n\ell} \mathbf{Bc} \tag{2}$$

where the Hamiltonian matrix $\mathbf{H}$ now looks as follows:

$$\mathrm{H_{ij}} = \frac{1}{2} \int_0^{r_{\max}} \frac{dB_{i,k}(r)}{dr} \frac{dB_{j,k}(r)}{dr} \, dr + \int_0^{r_{\max}} \left[\frac{\ell(\ell+1)}{2r^2} - \frac{Z}{r} + V_{ee}(r) \right] B_{i,k}(r) \, B_{j,k}(r) \, dr \tag{3}$$

and matrix $\mathbf{B}$ stays the same.

All integrals for both matrices are computed using Gaussian quadrature.

2.4 Self-Consistent Procedure

In self-consistent procedure, we update $V_{ee}(r)$ iteratively:

1. Start with $V_{ee}(r) = 0$.
2. Solve the generalized eigenvalue problem for all occupied orbitals.
3. Compute the radial charge density:

$$\rho(r) = \frac{1}{4\pi} \sum_j^{N_{occ}} N_j \left(\frac{P_{n_j \ell_j}(r)}{r} \right)^2 \tag{4}$$

where N_j is the occupation number.

4. Solve Poisson's equation with spherical symmetry:

$$\frac{1}{r}\frac{\partial^2\varphi(r)}{\partial r^2} = -4\pi\rho(r) \tag{5}$$

with boundary conditions $\varphi(0) = 0$ and $\varphi(r_{\max}) \to Z$.

Obtain, therefore, the potential:

$$V_{ee}^{\text{dir}}(r) = \frac{1}{r}\varphi(r) \tag{6}$$

where $\varphi(r)$ is expanded using B-splines and obtained via the collocation method just as in Assignment 4.

5. Add the Slater exchange potential:

$$V_{ee}^{\text{exch}}(r) = -3\left(\frac{3\rho(r)}{8\pi}\right)^{1/3} \tag{7}$$

and set:

$$V_{ee}^{\text{new}}(r) = V_{ee}^{\text{dir}}(r) + V_{ee}^{\text{exch}}(r) \tag{8}$$

6. Update the potential as follows:

$$V_{ee}^{\text{mixed}}(r) = (1-\eta)V_{ee}^{\text{new}}(r) + \eta V_{ee}^{\text{old}}(r) \tag{9}$$

where $\eta = 0.4$ controls convergence.

7. Repeat until all orbital energies $E_{n\ell}$ converge.

2.5 Total Energy and Ionization Energy

After convergence, we compute the total energy without double-counting the electron-electron interaction:

$$E_{\text{total}} = \sum_{i}^{N_{occ}} \left\{ E_{n\ell}^{i} - \frac{1}{2}\int_0^{r_{\max}} P_{n\ell}^{i}(r) V_{ee}(r) P_{n\ell}^{i}(r)\, dr \right\} \tag{10}$$

Ionization energies are obtained by computing the total energy difference between the neutral atom and the ionized one:

$$\Delta_{ion} = E_{total}^{neutral} - E_{total}^{ion}. \tag{11}$$

2.6 Analytical Solutions

We recall the analytical formula for obtaining the different energy levels:

$$E_n = -\frac{Z^2}{2n^2} \tag{12}$$

3 Results and Discussion

3.1 Convergence

Convergence of the self-consistent cycle is monitored by tracking changes in the orbital energies $E_{n\ell}$ between iterations. Convergence is assumed when the maximum change across all occupied orbitals falls below 10^{-6}.

3.2 Atomic Results

3.2.1 Helium and Helium Ion

The cycle converged after 16 iterations for **He** and after 2 iterations for the hydrogen-like solution. We used 30 knots before $r_{cut} = 2.0$ and 10 knots after with a domain $r \in (0, 5]$.

Orbital Energies and Total Energy. The hydrogen-like starting energy computed is -2.000 Hartree. After including electron-electron repulsion and exchange, the orbital energy shifts to -0.735 Hartree. The expectation value $\langle V_{ee} \rangle = 1.2335320988177276$ Hartree leads to a total energy of -2.704253 Hartree.

Radial Density and Normalization. The radial electron density, as seen in the figure below, shows a peak near the nucleus which is characteristic of a $1s$ orbital.

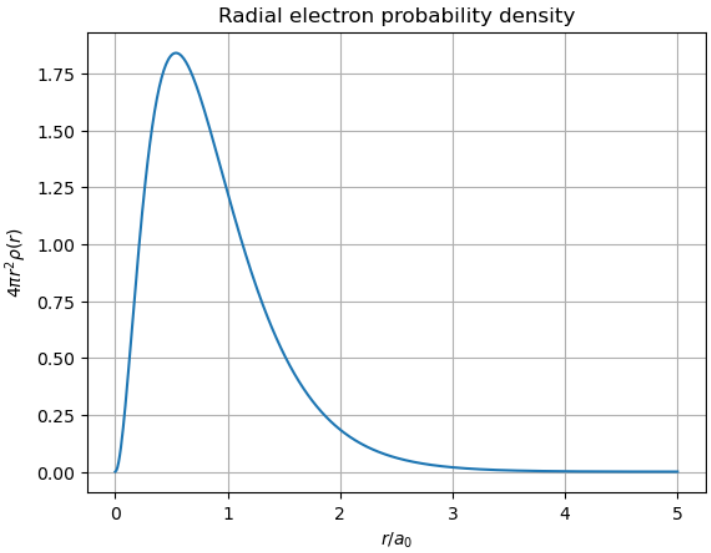

Figure 1: Radial electron probability density for **He**.

The normalization integral gives:

$$\int_0^\infty 4\pi r^2 \rho(r)\, dr = 2.00 \tag{13}$$

Potentials. The plots below show the difference between the direct potential obtained by solving Poisson's equation and the full electronic potential. In both graphs we can observe how the potential decays as $\frac{Z}{r}$ at large r.

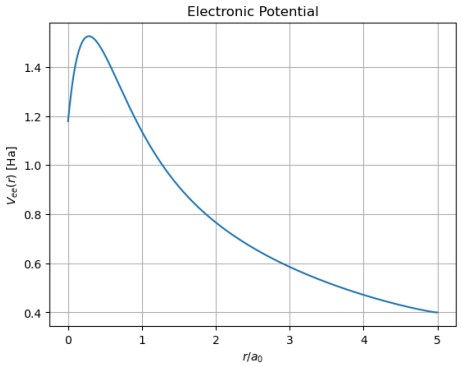

(a) Electronic potential for **He**.

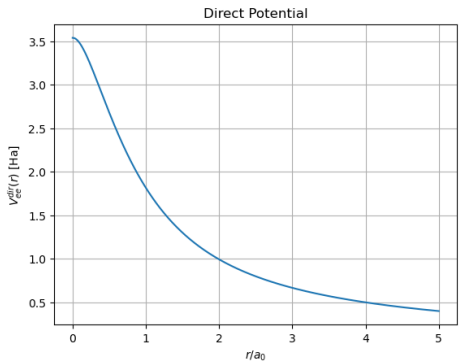

(b) Direct potential for **He**.

Figure 2: Both electronic and direct potentials for **He**.

Ionization Energy. The ionization energy obtained is:

$$\Delta_{\text{ion}} = E_{\text{He}^+} - E_{\text{He}} = -2.000 - (-2.704253) = 0.704253\,\text{Ha}. \tag{14}$$

3.2.2 Neon and Neon Ion

The cycle converged after 18 iterations for both **Ne** and $\mathbf{Ne}^+$. We used 70 knots before $r_{cut} = 2.0$ and 20 knots after with a domain $r \in (0, 3.5]$.

Orbital Energies and Total Energy. The obtained energies for **Ne** are as follows:

Orbital	$E_{n\ell}$ (Ha)	$\langle V_{ee} \rangle$ (Ha)	Occupation
1s	-31.4462	18.4867	2
2s	-1.5136	9.7163	2
2p	-0.6543	9.7935	6

Total energy:

$$E_{\text{total}} = -127.428956\,\text{Ha}. \tag{15}$$

And the obtained energies for $\mathbf{Ne}^+$ are:

Orbital	$E_{n\ell}$ (Ha)	$\langle V_{ee} \rangle$ (Ha)	Occupation
1s	-32.1093	17.8245	2
2s	-2.0041	9.4231	2
2p	-1.1429	9.6908	5

Total energy:

$$E_{\text{total}} = -125.415848\,\text{Ha}. \tag{16}$$

Radial Density and Normalization. Below we present the electron probability density for Neon where we now observe more than one peak.

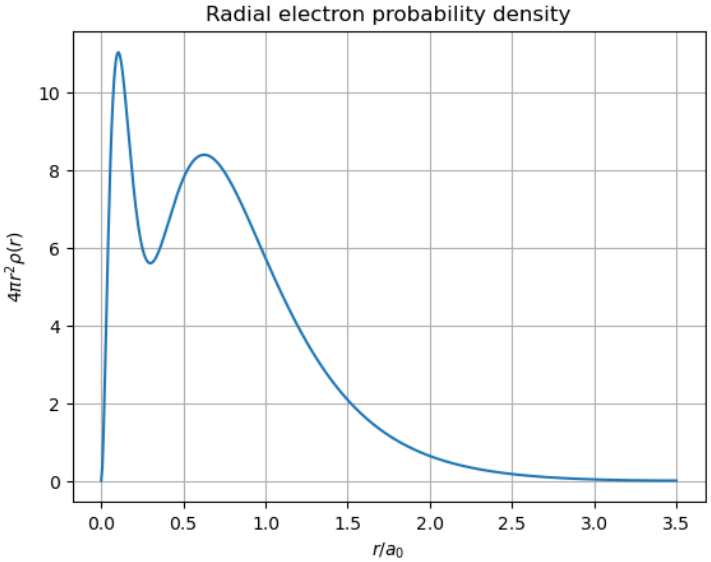

Figure 3: Radial electron probability density for **Ne**.

The normalization integral gives:

$$\int_0^\infty 4\pi r^2 \rho(r)\, dr = 10.00001 \tag{17}$$

Potentials. The plots below show the difference between the direct potential obtained by solving Poisson's equation and the full electronic potential. In both graphs, we can observe how the potential decays as $\frac{Z}{r}$ at large r.

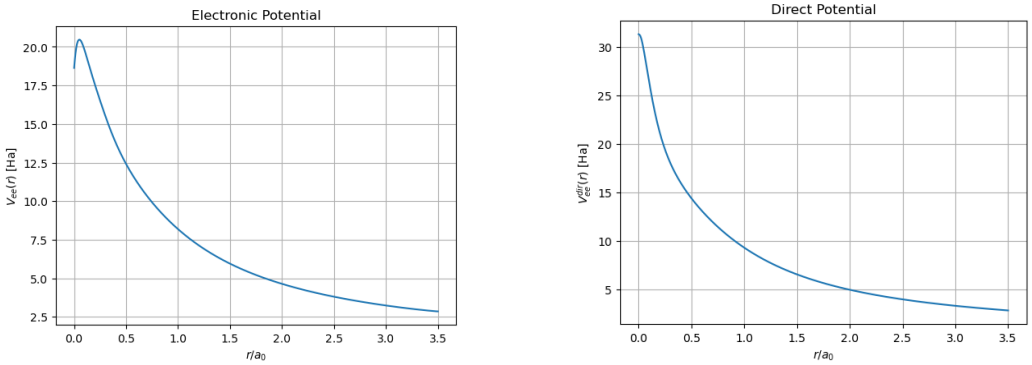

(a) Electronic potential for **Ne**.

(b) Direct potential for **Ne**.

Figure 4: Both electronic and direct potentials for **Ne**.

Ionization Energy. The ionization energy obtained is:

$$\Delta_{\text{ion}} = E_{\text{Ne}^+} - E_{\text{Ne}} = -125.415848 - (-127.428956) = 2.013108\,\text{Ha}. \quad (18)$$

We note how these results are clearly off to what we expected. By looking at the orbital and total energies for both **Ne** and $\mathbf{Ne}^+$ we observe how we fail to capture the results for $\mathbf{Ne}^+$ more than those of **Ne**.

3.2.3 Argon and Argon Ion

The cycle converged after 18 iterations for both **Ar** and $\mathbf{Ar}^+$. We used 100 knots before $r_{cut} = 2.0$ and 20 knots after with a domain $r \in (0, 4.5]$.

Orbital Energies and Total Energy. The obtained energies for **Ar** are as follows:

Orbital	$E_{n\ell}$ (Ha)	$\langle V_{ee} \rangle$ (Ha)	Occupation
1s	-116.4077	45.5047	2
2s	-11.3771	27.5867	2
3s	-1.0047	12.8955	2
2p	-9.0391	29.3518	6
3p	-0.4792	11.9689	6

Total energy:

$$E_{\text{total}} = -524.638088\,\text{Ha}. \quad (19)$$

From Eq.12 we see how the first orbital should have energy -162 Ha. By adding: $E^{1s}_{n\ell} + \langle V^{1s}_{ee} \rangle = -116.4077 - 45.5047 = -161.9124$ Ha, we get a value very closed to the original which may be and indication that our results are right.

The obtained energies for $\mathbf{Ar}^+$ are:

Orbital	$E_{n\ell}$ (Ha)	$\langle V_{ee} \rangle$ (Ha)	Occupation
1s	-116.7779	45.1346	2
2s	-11.7312	27.2387	2
3s	-1.2803	12.8726	2
2p	-9.3951	29.0045	6
3p	-0.7363	12.1423	5

Total energy:

$$E_{\text{total}} = -522.246189\,\text{Ha}. \quad (20)$$

Radial Density and Normalization. Below we present the electron probability density for Argon.

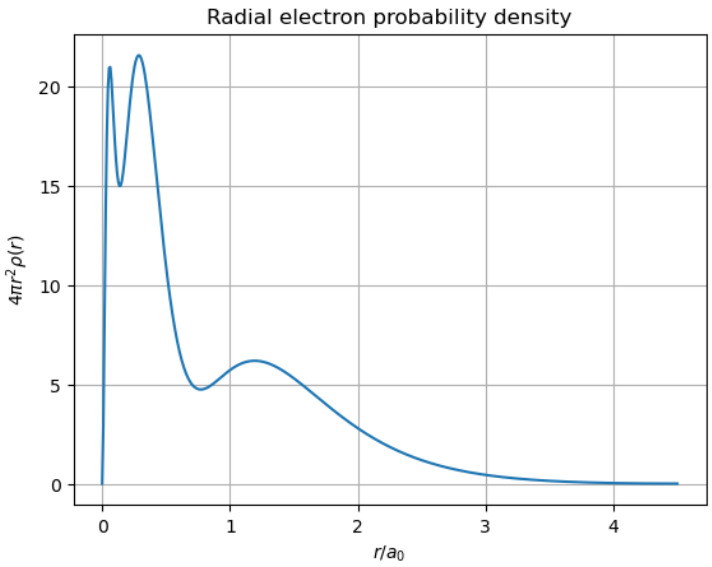

Figure 5: Radial electron probability density for **Ar**.

The normalization integral gives:

$$\int_0^\infty 4\pi r^2 \rho(r)\, dr = 18.00037 \tag{21}$$

Potentials. The plots below show the difference between the direct potential obtained by solving Poisson's equation and the full electronic potential. In both graphs, we can observe how the potential decays as $\frac{Z}{r}$ at large r.

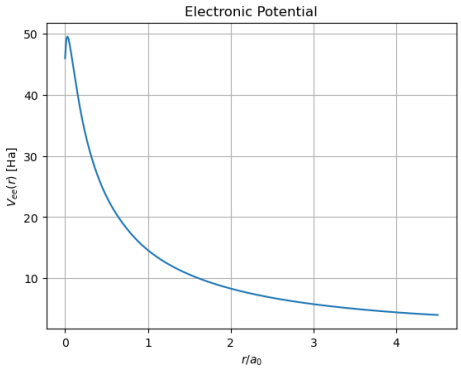

(a) Electronic potential for **Ar**.

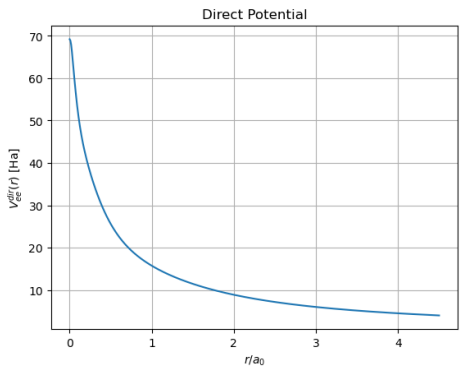

(b) Direct potential for **Ar**.

Figure 6: Both electronic and direct potentials for **Ar**.

Ionization Energy. The ionization energy obtained is:

$$\Delta_{\text{ion}} = E_{\text{Ar}^+} - E_{\text{Ar}} = -522.246189 - (-524.638088) = 2.391899\,\text{Ha}. \quad (22)$$

We note again how our value for the ionization energy is much more higher than it should be.

3.2.4 Potassium and Potassium Ion

The cycle converged after 18 iterations for both **K** and $\mathbf{K}^+$. We used 100 knots before $r_{cut} = 2.0$ and 20 knots after with a domain $r \in (0, 6.0]$.

Orbital Energies and Total Energy. The obtained energies for **K** are as follows:

Orbital	$E_{n\ell}$ (Ha)	$\langle V_{ee} \rangle$ (Ha)	Occupation
1s	-131.2267	49.2057	2
2s	-13.4666	30.0982	2
3s	-1.3980	14.5625	2
2p	-10.9305	32.0682	6
3p	-0.7887	13.7190	6
4s	-0.0117	6.2343	1

Total energy:

$$E_{\text{total}} = -596.854515\,\text{Ha}. \quad (23)$$

From Eq.12 we see how the first orbital should have energy -180.5 Ha. By adding: $E_{n\ell}^{1s} + \langle V_{ee}^{1s} \rangle = -131.2267 - 49.2057 = -180.4324$ Ha, we get a value

very closed to the original which may be and indication that our results are right.

When placing the last electron in the 3d orbital, the obtained energies for **K** are as follows:

Orbital	$E_{n\ell}$ (Ha)	$\langle V_{ee} \rangle$ (Ha)	Occupation
1s	−131.1379	49.2948	2
2s	−13.3552	30.2130	2
3s	−1.2961	14.5832	2
2p	−10.8213	32.1830	6
3p	−0.6930	13.6655	6
3d	−0.1153	9.0897	1

Total energy:

$$E_{\text{total}} = -596.730085\,\text{Ha}. \tag{24}$$

We observe how the orbital energy for 3d is higher than the one obtained for 4s. This is an indicator that placing the last electron in 3d is energetically unfavourable for potassium.

The obtained energies for $\mathbf{K}^+$ are:

Orbital	$E_{n\ell}$ (Ha)	$\langle V_{ee} \rangle$ (Ha)	Occupation
1s	−131.3693	49.0630	2
2s	−13.6081	29.9571	2
3s	−1.5343	14.4604	2
2p	−11.0721	31.9272	6
3p	−0.9214	13.6872	6

Total energy:

$$E_{\text{total}} = -595.308909\,\text{Ha}. \tag{25}$$

Radial Density and Normalization. Below we present the electron probability density for Potassium.

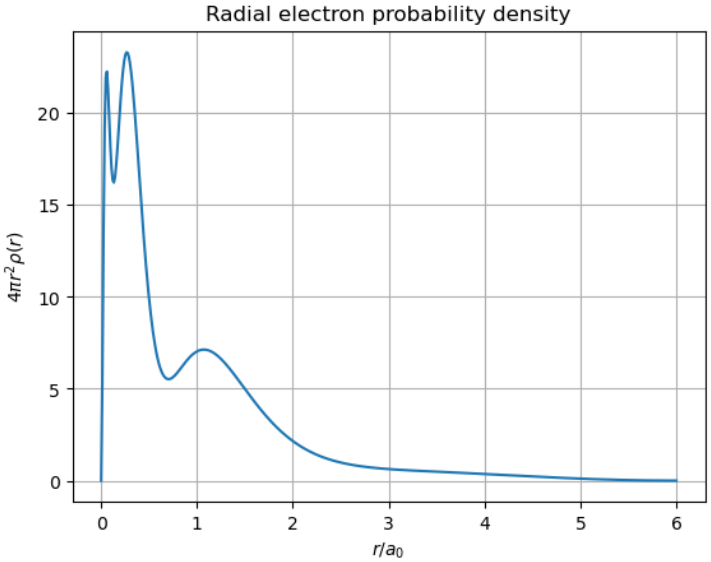

Figure 7: Radial electron probability density for **K**.

The normalization integral gives:

$$\int_0^\infty 4\pi r^2 \rho(r)\, dr = 19.00142 \tag{26}$$

Potentials. The plots below show the difference between the direct potential obtained by solving Poisson's equation and the full electronic potential. In both graphs, we can observe how the potential decays as $\frac{Z}{r}$ at large r.

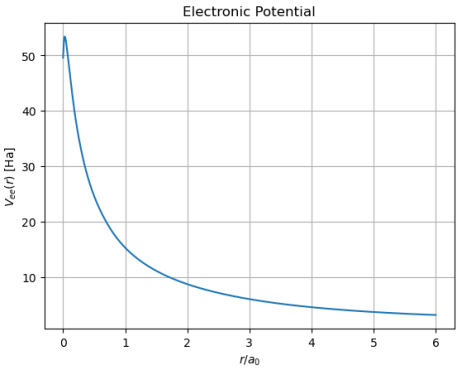

(a) Electronic potential for **K**.

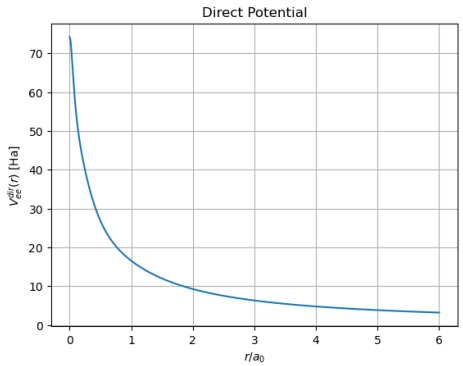

(b) Direct potential for **K**.

Figure 8: Both electronic and direct potentials for **K**.

Ionization Energy. The ionization energy obtained, placing the last electron in 4s, is:

$$\Delta_{\text{ion}} = E_{\text{K}^+} - E_{\text{K}} = -595.308909 - (-596.854515) = 1.545606\,\text{Ha}. \quad (27)$$

We again note how our value for the ionization energy is much more higher than it should be. Nevertheless, the value obtained is lower than those obtained for the noble gases.

4 Limitations of the Model

As we have observed, our model does not reproduce the results we were aiming for. Although achieving the expected values for **He** and close approximations for **Ne** (neutral), we fail to correctly reproduce ionization energies. Nevertheless, the plots obtained for the potentials and probability densities, as well as the normalization integrals, seem to align well with theory.

The failure in our implementation can be due to several approximations: the choice for the Slater potential, our knot sequence and choice of B-splines or not tuning the η parameter appropriately for each element.